

Defect concentration and Δn change in light- and elevated temperature-induced degradation

Moonyong Kim^{1,*} , Matthew Wright¹, Daniel Chen^{1,2}, Catherine Chan¹, Alison Ciesla¹, Malcolm Abbott¹ and Brett Hallam¹

¹ School of Photovoltaic and Renewable Energy Engineering, University of New South Wales, Sydney, New South Wales 2052, Australia

² Sundrive Solar, Kirrawee, 2232 NSW, Australia

E-mail: Moonyong.kim@unsw.edu.au

Received 29 June 2021, revised 2 September 2021

Accepted for publication 29 October 2021

Published 16 November 2021



Abstract

The wide variety of silicon materials used by various groups to investigate LeTID make it difficult to directly compare the defect concentrations (N_t) using the typical normalised defect density (NDD) metric. Here, we propose a new formulation for a relative defect concentration (β) as a correction for NDD that allows flexibility to perform lifetime analysis at arbitrary injection levels (Δn), away from the required ratio between Δn and the background doping density (N_{dop}) for NDD of $\Delta n/N_{\text{dop}} = 0.1$. As such, β allows for a meaningful comparison of the maximum degradation extent between different samples in different studies and also gives a more accurate representative value to estimate the defect concentration. It also allows an extraction at the cross-over point in the undesirable presence of iron or flexibility to reduce the impact of modulation in surface passivation. Although the accurate determination of β at a given Δn requires knowledge of the capture cross-section ratio (k), the injection-independent property of the β formulation allows a self-consistent determination of k . Experimental verification is also demonstrated for boron-oxygen related defects and LeTID defects, yielding k -values of 10.6 ± 3.2 and 30.7 ± 4.0 , respectively, which are within the ranges reported in the literature. With this, when extracting the defect density at different Δn ranging between 10^{14} cm^{-3} to 10^{15} cm^{-3} with $N_{\text{dop}} = 9.1 \times 10^{15} \text{ cm}^{-3}$, the error is less than 12% using β , allowing for a greatly improved understanding of the defect concentration in a material.

Keywords: light- and elevated temperature-induced degradation, crystalline silicon solar cells, defects in silicon, light-induced degradation, boron–oxygen defects

(Some figures may appear in colour only in the online journal)

1. Introduction

The normalised defect density (NDD) metric has been widely used to quantify the two common types of light-induced degradation (LID), boron oxygen related LID (BO-LID) [1, 2] and light and elevated temperature induced degradation

(LeTID) [3–6]. The NDD is calculated based on the difference in inverse effective lifetime (τ_{eff}) after ($\tau_{\text{eff},f}$) and before lifetime degradation ($\tau_{\text{eff},i}$) [7, 8]. It is important to note that the $\tau_{\text{eff},i}$ does not always mean the τ_{eff} before the light soaking since pre-formation of LeTID is known to occur without any illumination. However, in general, most of studies use $\tau_{\text{eff},i}$ as the τ_{eff} before light soaking. The influence due to pre-formed defect is generally not as significant as the total amount of defects due to subsequent light soaking. The NDD

* Author to whom any correspondence should be addressed.

is equivalent to the inverse of the Shockley–Read–Hall lifetime ($1/\tau_{\text{SRH}}$) equation [9] as follows:

$$\frac{1}{\tau_{\text{SRH}}} = \text{NDD} = \frac{p_0 + n_0 + \Delta n}{\tau_{p0}(n_0 + n_1 + \Delta n) + \tau_{n0}(p_0 + p_1 + \Delta n)}, \quad (1)$$

where τ_{n0} and τ_{p0} are the fundamental lifetimes of electrons and holes, respectively, and n_0 and p_0 are the equilibrium concentrations of electrons and holes, respectively. Equation (1) is valid when we assume that trapping [10] at a given Δn is negligible, such that the excess carrier concentrations of the electrons and holes are equal ($\Delta n = \Delta p$). n_1 and p_1 are electron and hole densities when the Fermi energy coincides with the recombination centre energy, respectively [11]. τ_{p0} and τ_{n0} are given by:

$$\tau_{n0} = \frac{1}{N_t \sigma_n v_{\text{th},n}} \text{ and } \tau_{p0} = \frac{1}{N_t \sigma_p v_{\text{th},p}} = \frac{k}{N_t \sigma_n v_{\text{th},p}}, \quad (2)$$

where they are determined by the concentration of the defect (N_t), capture cross-section of holes (σ_p) and electrons (σ_n), and the thermal velocity of electrons ($v_{\text{th},n} = 2.05 \times 10^7 \text{ cm s}^{-1}$) and holes ($v_{\text{th},p} = 1.69 \times 10^7 \text{ cm s}^{-1}$) at 300 K [12] and capture cross-section ratio, $k = \sigma_n/\sigma_p$. Combining and rearranging equations (1) and (2) for sufficiently high doping densities for p -type wafer ($N_{\text{dop}} \approx p_0 \gg n_0$) gives:

$$\text{NDD} = N_t \sigma_n \frac{N_{\text{dop}} + \Delta n}{\frac{k}{v_{\text{th},p}}(n_1 + \Delta n) + \frac{1}{v_{\text{th},n}}(N_{\text{dop}} + p_1 + \Delta n)}. \quad (3)$$

Therefore, when σ_n and σ_p of the specific defect of interest are known, the NDD or $1/\tau_{\text{SRH}}$ value can be used to identify N_t directly with different N_{dop} . However, when σ_n and σ_p are unknown, despite the known value of the ratio $k (= \sigma_n/\sigma_p)$, the absolute value of N_t cannot be identified. Therefore, NDD has been widely used to represent N_t , where NDD for the specific injection level and doping concentration is linearly proportional to N_t [13]. The NDD is also often defined as normalised defect concentration (N_t^*). However, equation (3) also shows that variations in the doping density (N_{dop}) and injection-level or excess carrier concentrations (Δn) result in significant variations in the calculated value of NDD. These variations also depend on the k of the defect.

Moreover, a thorough study highlighting the advantages and disadvantages of using NDD was recently presented by Herguth [8]. A key advantage of the NDD is that it allows quick comparison of the relative changes in the N_t for samples with an identical background doping density, N_{dop} . Another advantage is that no prior knowledge of the defect properties, such as the capture cross-section ratio, k , is required. The disadvantage is that by not taking k into account, the identical change in lifetime caused by a different defect with a different value of k is attributed to the same apparent defect concentration. Moreover, the NDD has an injection dependence where the value can vary for a given defect concentration. The variation is due to the change in recombination rate

with the number of electrons and holes, which is determined by the value of Δn for silicon with a given value of N_{dop} . The study showed the potential influence of the impact of additional recombination channel on NDD. This can be identified by extracting NDD at different Δn where NDD value can cross over in some Δn range.

In order for the NDD to be directly comparable in different samples, the NDD needs to be calculated based on an equal ratio of $\Delta n/(N_{\text{dop}} + N_{\text{dop}})$ [7]. In addition, the 2001 study by Glunz *et al* noted that other defect reactions should either not occur, or be comparably insignificant [7]. In order to address the former, calculations of NDD are typically performed using $\Delta n = 0.1 \times N_{\text{dop}}$, which is the assumption used by many studies on metastable defects of LeTID or BO-LID with an unknown σ_n of the defect for p -type substrates. This approach has been widely used to compare the defect concentration with different N_{dop} [7, 14]. However, some studies have extracted the lifetime at arbitrary Δn values that may have over- or underestimated the N_t based on the calculated NDD, which does not allow direct comparison among other studies, for example, in [3, 5, 15, 16]. Therefore, it is not possible to make direct comparison of the values. Considering the degradation rate for LeTID is linearly proportional to the generated Δn [17], the extraction of NDD from an arbitrary range of Δn and different N_{dop} does not allow easy comparison to estimate the variation of Δn during constant illumination. Moreover, the value of NDD can be influenced by iron, as discussed by Herguth [8]. To minimise this effect, the lifetime analysis should occur at the cross-over point to minimise the impact of iron.

When multiple reactions occur and induce recombination changes for more than one defect, especially changes in the surface lifetime, τ_{sur} , the defect concentration based on the NDD metric cannot be an accurate representation of N_t at a single Δn . Herguth proposed that using NDD at different Δn allows the determination of the presence of more than one defect [18]. However, the value of NDD at a single Δn can be influenced by other defects and the value is not directly comparable. Moreover, NDD can vary when different values of Δn [8] and N_{dop} are used. In the instance when there is a presence of only one defect, one approach to correct NDD with different ratio of Δn and N_{dop} for a comparison is by calculating NDD at different Δn using the known k for the same type of defect. Nevertheless, the NDD is not the best representation of N_t ; it does not necessarily allow for direct comparison among other studies, but rather provides a relative recombination rate that can be confounded by other defect interactions.

In this manuscript, we introduce the metric β for the relative defect concentration to provide a correction for NDD. The introduction of this formalism can overcome the dependencies of NDD on Δn and N_{dop} and minimise the influence due to other recombination by unwanted reactions. β can allow for direct comparison between various studies presented in the literature and be a more accurate representation. Furthermore, the theoretically Δn independent properties of β can be used to estimate defect parameters, such as the capture

cross-section ratio, k , providing another approach identifies the defect parameter. β is particularly helpful when studying LID effects of deep-level defects in crystalline silicon and to enable alternative approaches for comparisons between different studies of BO-LID and LeTID, especially related to defect kinetics. The paper first defines β and then derives the conversion equation from NDD into β . This is followed by a sensitivity analysis of the β metric, which demonstrates an advantage when directly comparing different samples without knowing other dependencies such as Δn .

2. The relative defect concentration and the conversion from NDD

The relative defect concentration, β , as the product of the true defect concentration (N_t) and the capture cross-section of electrons (σ_n) is given by:

$$\beta = N_t \sigma_n. \quad (4)$$

Since defects are often studied with unknown σ_n and σ_p values, the NDD (equation (3)), k and equation (4) can be combined such that β can be expressed as:

$$\beta = \left(\frac{\Delta n + n_1}{N_{\text{dop}} + \Delta n} \frac{k}{v_{\text{th},p}} + \frac{N_{\text{dop}} + \Delta n + p_1}{N_{\text{dop}} + \Delta n} \frac{1}{v_{\text{th},n}} \right) \text{NDD}. \quad (5)$$

Thus, NDD can be converted to β , to account for differences in the dependent values (Δn and N_{dop}). This can be simplified using typical conditions and assumptions. At 300 K, for p -type silicon with sufficiently high doping densities ($N_{\text{dop}} > 10^{15} \text{ cm}^{-3}$) and minority carrier concentrations, such that $N_{\text{dop}} (\approx p_0)$, $\Delta n \gg n_1$, p_1 , and N_{dop} and $\Delta n > 1 \times 10^{12} \text{ cm}^{-3}$ for deep level defects, such that equation (5) can be rearranged and simplified to β as follows:

$$\beta \approx \left(\frac{\Delta n}{N_{\text{dop}} + \Delta n} \times \frac{k}{v_{\text{th},p}} + \frac{1}{v_{\text{th},n}} \right) \text{NDD}. \quad (6)$$

As samples with $N_{\text{dop}} \gg n_1, p_1$ are used, the simplified version is used for converting from NDD or τ_{SRH} to β unless otherwise specified. Unlike NDD, accurate determination of β for given Δn and N_{dop} values requires additional information about the value of k . However, the k of defects such as BO-LID and LeTID are typically known; hence this does not present a significant issue for a study of one defect. Furthermore, when unknown, the actual value of k can be found by using injection-level dependent lifetime data using equation (6), which will be discussed in section D. Moreover, when the k of a defect is known, β provides an essential correction of NDD to a given injection level.

2.1. Conversion of NDD to β with different Δn and N_{dop}

This section presents the conversion from NDD to β using simulated values to demonstrate the theoretical advantage of β . NDD values with different Δn and N_{dop} values are calculated

based on equation (3) and plotted in figure 1(a). The input value of $N_t \sigma_n = 10^{-3} \text{ cm}^{-1}$ is used. This is equivalent to the defect concentration, $N_t = 10^{11} \text{ cm}^{-3}$ and $\sigma_n = 10^{-14} \text{ cm}^2$, for example. The value of T and k used in the simulation is 300 K and 35, respectively, which is based on a study by Niewelt *et al* for recombination caused by LeTID [21] for mid-gap level defects. When the ratio of Δn and N_{dop} is the same, the NDD is identical, which allows a direct comparison of N_t with different N_{dop} . This is the approach many studies have used to apply NDD as first proposed in [1] correctly. However, this practice was not always applied in all studies, such that the NDD values are not directly comparable among studies. For instance, using $\Delta n = 0.1 \times N_{\text{dop}}$ may not always be suitable, such as in the presence of iron. This can be overcome when Δn is extracted at the cross-over point [26], which has been demonstrated in our previous study [27], but then the ratio of Δn and N_{dop} may no longer be the same with different N_{dop} values.

There are discrepant ratios of $\Delta n/(N_{\text{dop}} + \Delta n)$ that have been used to extract NDD by others, which are depicted in symbols [3, 6, 15, 21–23, 28]. The figure shows that for a given true defect concentration, the NDD would vary by more than an order of magnitude simply due to the range of Δn and N_{dop} values that were used in those studies. As such, NDD values cannot be directly compared. The calculated value of NDD is only identical when the ratio of $\Delta n/(N_{\text{dop}} + \Delta n)$ is equal. If this is not the case, then the assumption of $\text{NDD} \propto N_t$ [7] is invalid, and any studies that do not follow the ratio are not comparable. Therefore, the value of NDD will always require additional information of Δn and N_{dop} to ensure comparability between different studies. As such, the absolute value of NDD is meaningless without information on the Δn and N_{dop} , although such values should also be known and presented. When an incorrect ratio is used, a conversion is required to enable comparison between different studies.

Using equation (6), the NDD is converted to β with different input values of Δn and N_{dop} . If we compare this to an assumed reference value of β , $\beta_{\text{ref}} = N_t \sigma_n = 10^{-3} \text{ cm}^{-1}$, for example, we can see in figure 2(b) that β is almost identical to β_{ref} with different N_{dop} and Δn values, unlike the NDD values. The error at low N_{dop} is when n_1 and p_1 are similar to N_{dop} and the error is still less than 5%. Note that this error value may vary based on defect property such as k , but this error can typically be ignored since N_{dop} values for silicon wafers in the photovoltaics industry is well above 10^{14} cm^{-3} . As such, the error is expected to be negligible for solar cell applications. The symbols of examples all lie well within the range where β is unchanged, which indicates that the value of NDD from those studies can be converted to β to make direct comparisons on the concentration of N_t in the different materials.

2.2. Sensitivity analysis—the impact of input k on β

While β has an advantage over NDD, such as a single value being obtained regardless of N_{dop} or Δn , a potential disadvantage of using β compared to NDD is that an input value of

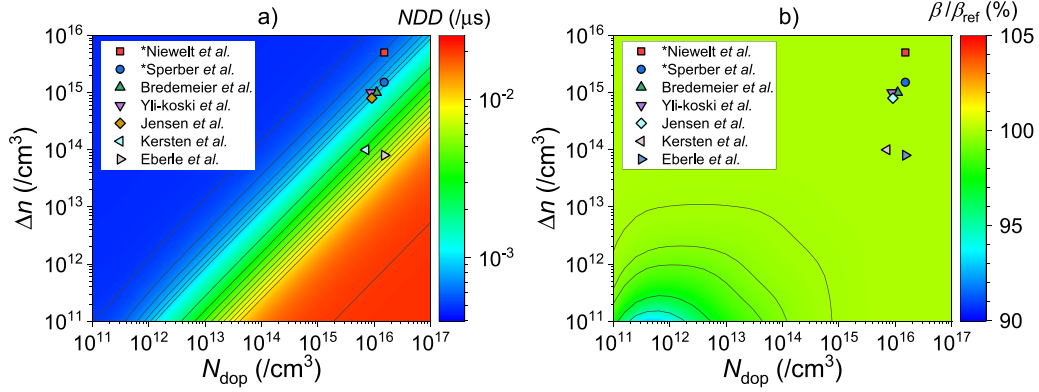


Figure 1. Plots of simulated results of (a) normalised defect density (NDD) and (b) the converted value of relative defect concentration, β , using equation (6) with $k = 35$ to the reference value of β , β_{ref} (β/β_{ref}) as a function of doping density, N_{dop} in p -type silicon, and excess minority carrier concentrations, Δn . The symbols on the graphs show Δn where effective lifetimes (τ_{eff}) were extracted to calculated NDD and N_{dop} that are used in the studies of LeTID [3, 6, 15, 21–23, 28]. * indicates that the study only reported τ_{eff} .

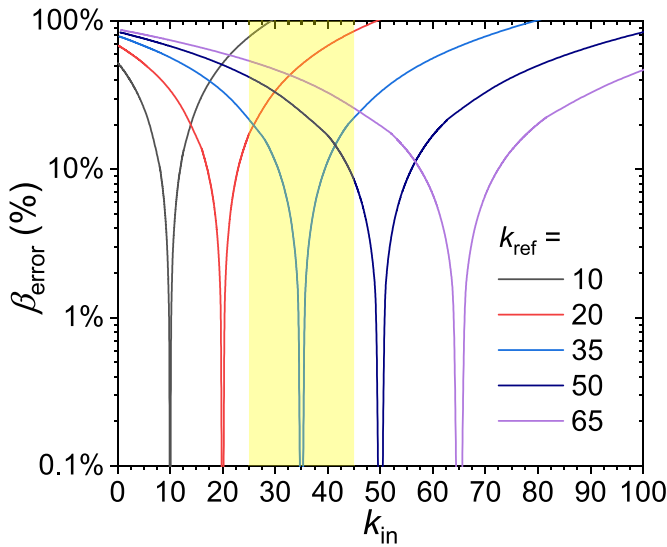


Figure 2. The error of (β_{error}) calculated from the reference value of β (β_{ref}) as a function of input capture cross-section ratio, k_{in} with different reference k values (k_{ref}) where β is calculated at $\Delta n/N_{\text{dop}} = 0.1$ with $N_{\text{dop}} = 10^{16} \text{ cm}^{-3}$. The highlighted region indicates the $k = 35 \pm 10$.

k is required for equations (5) or (6). Therefore, the accurate determination of β for a given Δn value requires knowledge of the correct value of k . k values are usually widely reported in the literature. However, a large range of k values has been reported for some defects such as that responsible for LeTID; with k values ranging from around 20 [21, 24, 29] to above 60 [30], although the value typically lies in the range between 20 and 40 [21, 24, 31]. For BO defects, the k -value is around 10–20 depending on whether it is assumed to be a single defect or two defects [1, 2, 32, 33].

As such, due to variations in the value of k reported, it is important to understand the sensitivity of β to different input k values, and hence errors of k . A sensitivity analysis of the β calculation on k is performed by varying the input k value (k_{in}) using the simulated τ_{SRH} at 300 K and $\beta_{\text{ref}} = 10^{-3} \text{ cm}^{-1}$ to

determine the error in β , β_{error} , for different reference k values (k_{ref}). That is, k_{ref} is the correct k value. For simplicity, β was calculated based on τ_{SRH} at $\Delta n/N_{\text{dop}} = 0.1$.

Figure 2 shows that as k_{in} deviates further from k_{ref} , $\beta_{\text{error}} = (\beta - \beta_{\text{ref}})/\beta_{\text{ref}}$, increases. However, using $k_{\text{ref}} = 35$ as an example, considering the highest (60) and the lowest value (20) of k reported for LeTID, the error is, at most 50%. In comparison, NDD can have a much more significant range, with over an order of magnitude variation due to Δn from 10^{14} cm^{-3} to 10^{16} cm^{-3} with $N_{\text{dop}} = 10^{16} \text{ cm}^{-3}$ (for example, refer back to figure 1(a)).

While it is possible that an inaccurate value of k may make it challenging to use β to represent N_{t} , the error is still limited. In addition, k is known for most defects or is relatively easy to find by analysing injection-dependent lifetime curves, most generally in the inverse lifetime space. Furthermore, this information should be provided in manuscripts to increase the confidence of the defect responsible for the observations.

2.3. Using β to enable meaningful comparisons across studies

By converting NDD to β , it is possible to compare the relative N_{t} with any N_{dop} or Δn . The metric can, therefore, be used to compare the maximum degradation extent (MDE) from different studies. In figure 3, the MDE in terms of NDD (NDD_{MDE}) from some LeTID studies [6, 15, 19–21, 24, 25, 34] is converted to β (β_{MDE}). The details of the measurements used are in table 1, and the k_{in} is assumed to be 35 ± 10 . Most of the studies [15, 19, 20, 22, 23, 25, 34] did not report the k while other studies [6, 21, 24] reported slightly different value of k but since they are a study of LeTID defect in particular, the use of k_{in} as 35 ± 10 is valid. Ideally, the reported value k from each literature should be used but since the sensitivity is not so significant as shown in figure 2, 35 ± 10 was used for a simplicity. While many studies followed the rule using $\Delta n = 0.1 \times N_{\text{dop}}$ for NDD extraction (red dashed oval), there are other studies that did not follow this rule, which does not allow a direct comparison of the NDD_{MDE} values to other studies. The results that were done without illumination showed lower NDD_{MDE}

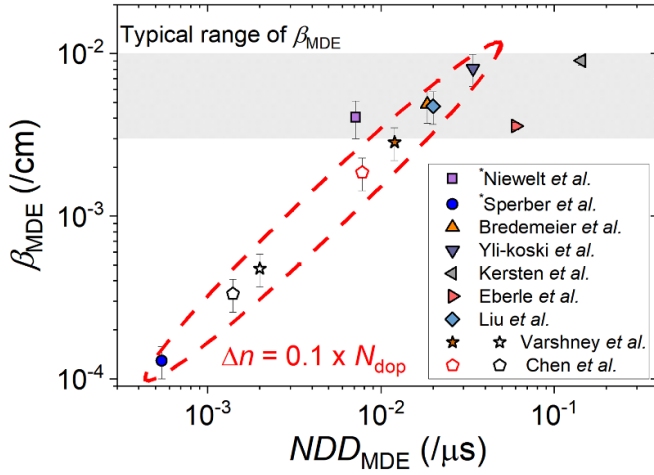


Figure 3. The normalised defect density at maximum degradation extent (NDD_{MDE}) from the literature [6, 15, 21–23, 25] versus relative defect concentration, β_{MDE} , which is calculated based on the minority carrier concentrations and background doping density with assumed k of 35 ± 10 . Error is based on the error of k . The red dashed oval indicates the studies that reported $\Delta n = 0.1 \times N_{dop}$. Open symbols were degraded without illumination.

[19, 24], which varied with the firing temperatures. The different values of NDD_{MDE} show it can be varied with different firing temperatures, testing condition, degradation and recovery rates or the pre-annealing condition. However, despite the values of NDD_{MDE} varying by more than one order of magnitude across the several different studies [6, 15, 23, 25, 35] due to different input values of $\Delta n/N_{dop}$, β_{MDE} , in contrast, typically lay within the range of $\sim(3-10) \times 10^{-3} \text{ cm}^{-1}$. The agreement shows that β should be a more accurate value after Δn and N_{dop} correction. The small variations of β may indicate that the relative concentration of LeTID related defects observed in various studies are far more similar than was previously possible to identify using the NDD metric without correction.

In particular, it is unclear why the β_{MDE} result from Sperber *et al* was significantly lower than other values. It could be caused by any of the following: a multitude of different wafer sources; processing recipe or layers ($\text{SiN}_x\text{:H}$ or Al_2O_3); peak firing temperature; phosphorus diffusion; or the testing condition. Nevertheless, the correct conversion to β , which is independent of Δn , showed the difference of the actual defect concentration at the MDE based on β_{MDE} of the two studies [21, 22] ($1 \Omega \text{ cm}$ with peak temperature of 900°C and $1 \Omega \text{ cm}$ with peak temperature of 800°C without corona charge, respectively) should be a factor of 30, rather than a factor of 13 when it is based on the value of NDD. The ability to meaningfully compare MDE in this way demonstrates that the difference in N_t between the studies is larger than it would have been calculated using NDD. With NDD alone, it was unrecognised that this result is significant and deserves more investigation to understand why it differs as part of the search for the specific defect and behaviour causing LeTID. This shows an example of the advantage of β , which is equivalent to a Δn -corrected NDD, where the value

is directly comparable and also convertible under different conditions.

2.4. Identifying the capture-cross section ratios using the β formulation

While an inaccurate value of k_{in} can result in an error in the calculated β at a given Δn , the formulation of β (equation (5)), its theoretically injection-level independent property, can, in fact, be used to identify the k -value for deep-level defects. This approach is similar to the other approaches by Murphy *et al* [36], which estimate capture coefficient, Q (similar to k) based on the linear slope over the normalised electron concentration over holes (n/p) for p-type. The approach shown here is based on the independence of Δn and β . When the correct k_{in} is used (i.e. $k_{in} = k_{ref}$), the calculated β will be equal at all Δn , provided that no other changes in lifetime occur. Figure 4(a) shows the NDD and calculated β for a reference k (k_{ref}) of 35, as a function of Δn normalised to N_{dop} ($\Delta n/N_{dop}$) with different k_{in} (10, 20, 35, 50, and 65). For the normalised range of Δn when N_{dop} and $\Delta n \gg n_1, p_1$, β formulation to identify k is applicable for any range of N_{dop} . The NDD is the theoretical result at $T = 300 \text{ K}$. NDD varies over a factor of 10 between $\Delta n/N_{dop} = 10^{-3}$ and 1. Note that this error varies even more significantly for defects with higher k_{ref} (see figure 2(b)). When $k_{in} = k_{ref}$, the calculated β is constant and equal to β_{ref} over the full range of $\Delta n/N_{dop}$ values, which shows β is independent of Δn . When k_{in} is incorrect (i.e. $k_{in}^1 \neq k_{ref}$), however, β varies as a function of Δn . Therefore, one advantage of β is the injection-level independent properties of the β formulation can provide an opportunity for a self-consistent determination of k . This variation of β over Δn with different k_{in} can be used as an indication to identify k_{ref} , by calculating the standard deviation χ_β as a function of Δn and k , as follows:

$$\chi_\beta = \sqrt{\frac{\sum_{i=1}^{N_m} (\beta_{\Delta n} - \beta_k)^2}{N_m - 1}}, \quad (7)$$

where N_m = the number of Δn measurements, β_k = mean of β with given k , $\beta_{\Delta n}$ = the calculated β as a function of Δn with given k . χ_β , as a function of k_{in} is shown in figure 4(b). The χ_β converges to the minimum value when k_{in} approaches k_{ref} . Therefore, based on the k that correlates with the minimum of χ_β , an optimised k (k_{opt}) of unknown defects can be found.

2.5. Sensitivity analysis due to other changes and improved approach using weighted values

When NDD is calculated based on the change in lifetime, it is assumed that the background lifetime does not change after defect formation (see equation (1)). That is, it is assumed that only one recombination mechanism (due to the defect of interest), is modulated. This assumption also applies when other fitting methods are used to identify the defect parameters [36, 37]. However, if the background lifetimes, τ_{BG} are also

Table 1. Details of the studies that are used as examples in figure 1.

Reference	Year published	Light soaking condition/time at MDE	Peak firing temperature	Sample resistivity and type	Δn (cm ⁻³)	$\Delta n/N_{\text{dop}}$
Yli-koski <i>et al</i> [6]	2019	80 °C + 0.6 sun/~30 h	835 °C	1.3 Ω cm mc-Si	1.14×10^{15}	0.1
Varshney <i>et al</i> [19]		130 °C + 26.6 kW m ⁻² /100 s	770 °C	1.6 Ω cm mc-Si	9.1×10^{14}	
Varshney <i>et al</i> [19]		175 °C/7 h				
Liu <i>et al</i> [20]	2018	75 ± 5 °C + 1 sun/140 h				
Niewelt <i>et al</i> [21]	2017	75 ± 5 °C + 1 sun/~5.5 h	900 °C	1 Ω cm FZ-Si	5×10^{15}	^a 0.33
Sperber <i>et al</i> [22]		80 °C + 1 kW m ⁻² /~1 h	800 ± 10 °C		1.5×10^{15}	0.1
Bredemeier <i>et al</i> [23]		75 °C + 0.5 sun/~150 h	788 ± 10 °C	1.66 Ω cm mc-Si	1×10^{15}	^a 0.087
Chen <i>et al</i> [24]		175 °C/~5 h	744 °C	1.6 Ω cm mc-Si	9.1×10^{14}	0.1
Chen <i>et al</i> [24]			815 °C			
Kersten <i>et al</i> [25]	2016	75 °C + 0.3 kW m ⁻² /~1100 h	—	1–2 Ω cm mc-Si	1×10^{14}	^a 0.015–0.072
Eberle <i>et al</i> [15]		75 °C + 1 sun/~106 h	800 °C	1.0 Ω cm mc-Si	8×10^{13}	^a 0.0053

^a indicates the $\Delta n/N_{\text{dop}}$ was calculated based on reported wafer resistivity, which was converted to the background doping density (N_{dop}), and minority carrier concentrations, Δn . All studies used p-type. MDE stands for maximum degradation extent.

changing due to other effects $\Delta\tau_{\text{other}}$, this can be expressed as follows:

$$\frac{1}{\Delta\tau_{\text{other}}} = \frac{1}{\tau_{\text{BG,BD}}} - \frac{1}{\tau_{\text{BG,AD}}}, \quad (8)$$

where $\tau_{\text{BG,BD}}$ and $\tau_{\text{BG,AD}}$ are the background lifetimes before and after degradation, respectively. Therefore, when $\Delta\tau_{\text{other}} \neq 0$, it can vary the apparent values of k (k_{app}), NDD (NDD_{app}), and β (β_{app}). The influence of $\Delta\tau_{\text{other}}$ on the apparent values of NDD, β , and k_{opt} is now demonstrated theoretically. The method will be implemented on experimental results in the later section. Here, the influence of $\Delta\tau_{\text{other}}$ is demonstrated based on a change in surface lifetime, τ_{sur} as an example. τ_{sur} can be quantified as:

$$\frac{1}{\tau_{\text{sur}}} = \frac{J_{0,e}}{qn_i^2 w} (N_{\text{dop}} + \Delta n), \quad (9)$$

where $J_{0,e}$ is the emitter saturation current density and w is the thickness of the silicon wafer. A change in τ_{sur} is a typical example that can influence the calculation of k (k_{app}) as surface passivation can be modulated during thermal treatments or light soaking, this modulation is injection dependent (τ_{sur} is lower at higher Δn). With an increase ($\Delta\tau_{\text{other},1}$) and decrease ($\Delta\tau_{\text{other},2}$) in emitter saturation current density, $J_{0,e}$ by 15 fA cm⁻², figure 5(a) shows NDD_{app} and NDD_{ref} as a function of $\Delta n/N_{\text{dop}}$ with k_{ref} of 35. NDD_{app} is calculated based on the sum of NDD_{ref} and $1/\Delta\tau_{\text{other}}$ ($\text{NDD}_{\text{app}} = \text{NDD}_{\text{ref}} + 1/\Delta\tau_{\text{other}}$) where NDD_{ref} is the reference NDD from figure 4(a). Input values $N_{\text{dop}} = 10^{16}$ cm⁻³ at $T = 300$ K are used for the calculation. Figure 5(b) shows the ratio of NDD_{app} to NDD_{ref} to highlight the impact of $\Delta\tau_{\text{other}}$. While $\text{NDD}_{\text{app},1}$ and $\text{NDD}_{\text{app},2}$ looked relatively similar compared to NDD_{ref} , the variation due to $\Delta\tau_{\text{other}}$ becomes more significant at a higher $\Delta n/N_{\text{dop}}$. This is to be expected for a deep-level defect which has smaller NDD magnitude at higher $\Delta n/N_{\text{dop}}$ [8], and due to a surface effect that has larger impact at higher $\Delta n/N_{\text{dop}}$ and should be taken into consideration. This

is also the reason why extracting NDD at $\Delta n = 0.1 \times N_{\text{dop}}$ can be disadvantageous. To minimise the influence of $\Delta\tau_{\text{other}}$, it would be generally recommended to use lower Δn where τ_{SRH} is more significant comparing to the lifetimes of other recombination components such as τ_{sur} .

One approach to minimise the influence of $\Delta\tau_{\text{other}}$ is by estimating k -value based on the different range of injection dependent NDD weighted towards the lower $\Delta n/N_{\text{dop}}$ range. Based on the results from figure 5(a), χ_{β} as a function of k_{in} with different fitting range is shown in figure 6(a). For NDD_{ref} , regardless of the range of $\Delta n/N_{\text{dop}}$, the minimum χ_{β} occurred at the k_{ref} . In comparison, $\text{NDD}_{\text{app},1}$ and $\text{NDD}_{\text{app},2}$ showed a significant difference with the different ranges. Using the k_{opt} with $\Delta n/N_{\text{dop}}$ range $\leq 10^{-1}$, the β as a function of $\Delta n/N_{\text{dop}}$ are shown in figure 6(b). It shows the β can also be varied at higher $\Delta n/N_{\text{dop}}$ due to change in τ_{sur} . However, in the lower range of $\Delta n/N_{\text{dop}}$ ($<10^{-1}$) where τ_{SRH} dominates, the variation of β is less significant. The influence of τ_{sur} can also vary the NDD value since identifying the τ_{SRH} as a function of Δn by subtracting the measurement before and after the degradation requires the assumption that only one type of defect is induced. In terms of the potential influence of iron as Herguth proposed [8], it can be taken into consideration by quantifying the concentration of iron, or the impact can be avoided or minimised by keeping the sample in the dark for a duration based on the N_{dop} and T to allow the association of iron and boron [38].

The simulated result in figure 6(b) suggests averaging the β in the lower range of $\Delta n/N_{\text{dop}}$ or selecting the $\Delta n/N_{\text{dop}}$ can allow an estimation of the defect concentration with less influence of $\Delta\tau_{\text{other}}$. It is possible that the change in τ_{bulk} or the presence of other types of LID can influence the lifetime in lower range of $\Delta n/N_{\text{dop}}$. However, the samples should be carefully prepared to avoid the influence of other types of LID in the first place. While k_{opt} was more accurate, the trend of β was not linear. However, this is due to $\Delta\tau_{\text{other}}$ that does not necessarily imply an incorrect k . Moreover, figure 7 summarises the $k_{\text{opt}}/k_{\text{ref}}$ ratio with different maximum ranges of $\Delta n/N_{\text{dop}}$

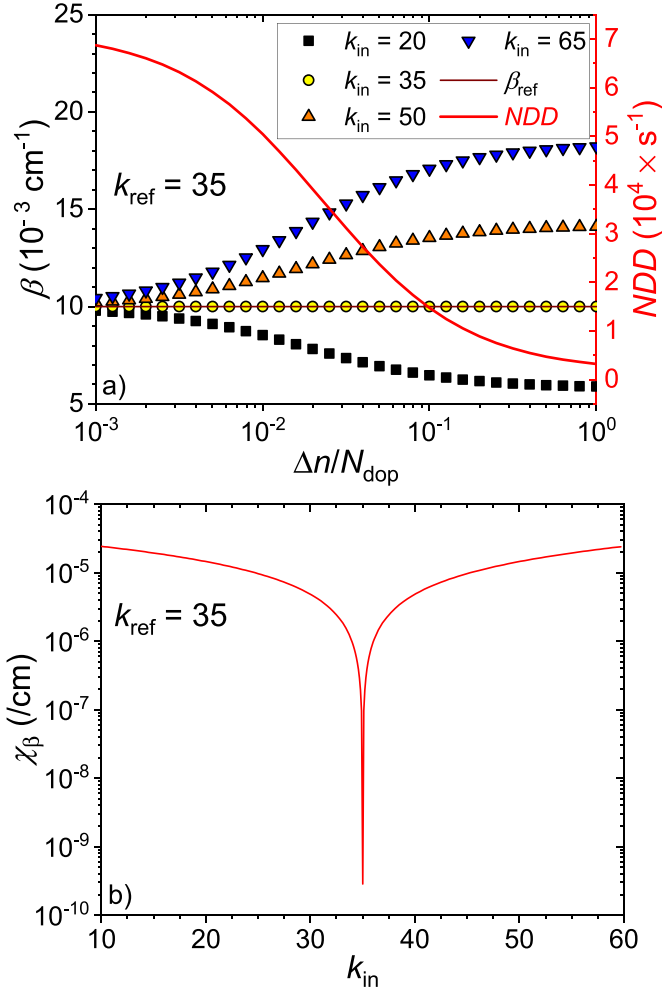


Figure 4. (a) The relative defect concentration, β as a function of normalised minority carrier concentrations over background doping density, $\Delta n/N_{\text{dop}}$ with different input k , k_{in} (10, 20, 35, 50, and 65) with reference k , k_{ref} of 35. Figure(b) shows the standard deviation of β , χ_{β} as a function of k_{in} .

(max $\Delta n/N_{\text{dop}}$) from $\Delta n/N_{\text{dop}} = 10^{-3}$. For NDD_{ref} , despite the range, k_{opt} was always equal to k_{ref} ($k_{\text{opt}}/k_{\text{ref}} = 1$).

It is possible that there are some instances where both BO-LID and LeTID are present [39, 40]. However, samples can be carefully prepared based on the characteristics of the each type of LID [40]. Our previous study showed that depending on the period where one of the two types of LID dominates, the k of each type can be carefully calculated to eliminate or minimise the influence of each other. Moreover, the presence of multiple types of LID can lead to change in the apparent value of k over time [27], which can, therefore, be considered or potentially isolated. Any fitting approach like Murphy *et al* [36] that uses residual of the measurement with and without the presence of a defect can potentially have this problem. Moreover, iron-related LID changes can be easily avoided or isolated by resting the sample in the dark to allow the complete association of iron and boron-based on the T and N_{dop} [38]. Therefore, for deep level defects, the lower range of $\Delta n/N_{\text{dop}}$ will give a more accurate k with the minimum influence of τ_{sur} . Moreover, such

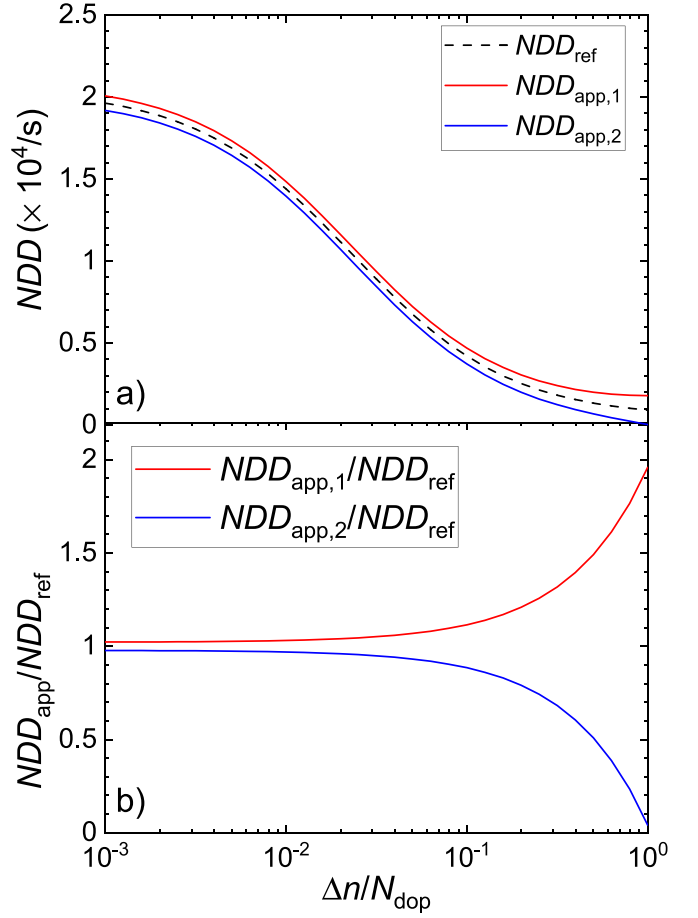


Figure 5. (a) The normalised defect density (NDD), with the influence of $\Delta\tau_{\text{other}}$ ($NDD_{\text{app},1}$ or $NDD_{\text{app},2}$) as a function of $\Delta n/N_{\text{dop}}$. NDD_{ref} is the reference value. (b) Ratio of $NDD_{\text{app},1}$ or $NDD_{\text{app},2}$ over NDD_{ref} as a function of $\Delta n/N_{\text{dop}}$.

evidence of giving different k_{opt} with different ranges of Δn indicates the influence of $\Delta\tau_{\text{other}}$.

The $NDD_{\text{app},1}$ and $NDD_{\text{app},2}$ showed a decrease and increase in $k_{\text{opt}}/k_{\text{ref}}$, respectively, where the error range increased with higher $\Delta n/N_{\text{dop}}$ values. The implication is that in order to reduce the error due to $\Delta\tau_{\text{other}}$, one approach is to select a lower $\Delta n/N_{\text{dop}}$ range. Additionally, the difference in k_{opt} with $\Delta n/N_{\text{dop}}$ range implies there are other changes. It is important to consider, however, the other typical error such as depletion-region modulation effect [41] or trapping artefacts [42] at the lower range. So, while it is recommended to select the lower range, it is also important to exclude those ranges to estimate k accurately. Nevertheless, whether there is an influence of $\Delta\tau_{\text{other}}$ or not, k_{opt} will be more accurate with a lower range above the artefact range.

A summary of the decision diagram of β method to estimate k based on k_{opt} is shown in figure 8. For shallow defects where n_1 and p_1 are significant to N_{dop} and Δn unless E_t is known, this approach cannot be used. The study will use two common and detrimental deep-level defects due to BO-LID and LeTID with N_{dop} values typical for silicon solar cells, so the approach will not be limited to the property of the defects.

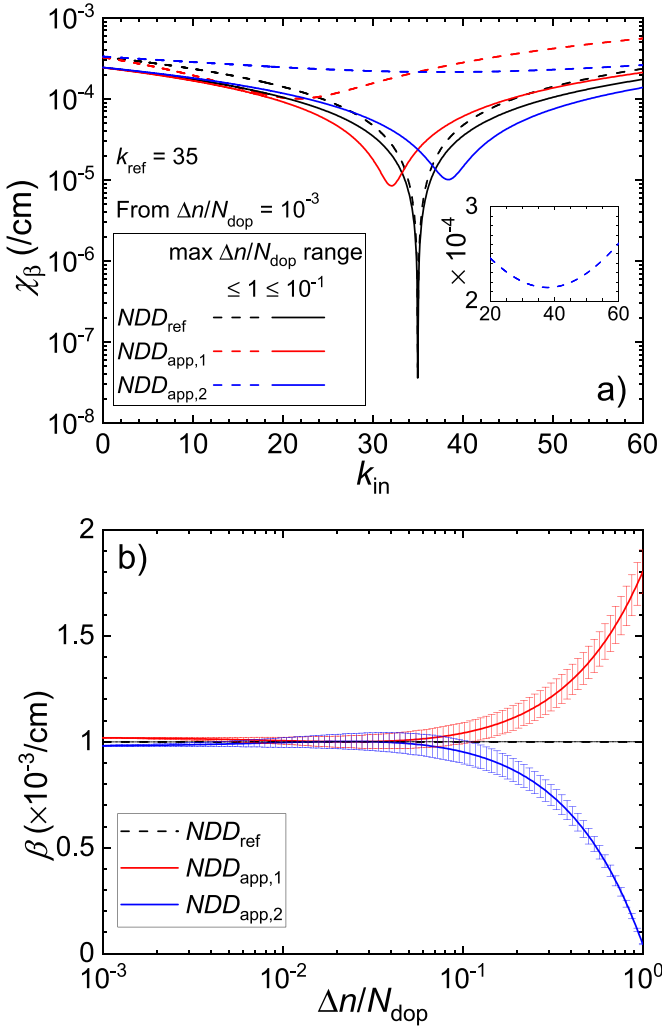


Figure 6. (a) Standard deviation, χ_β as a function of input k , k_{in} , which is calculated at the different $\Delta n/N_{dop}$ ranges. (b) Relative defect concentration, β as a function of $\Delta n/N_{dop}$ on NDD_{ref} , $NDD_{app,1}$, and $NDD_{app,2}$. Inset in (a) shows different ranges.

2.6. Converting β to carrier lifetime as a function of Δn

While inverse τ_{SRH} is equal to NDD, the NDD is typically used to only represent the recombination rate at a given Δn only. β is equal to $N_t \sigma_n$ in comparison (equation (2)) such that generating a lifetime curve over the range of Δn is straightforward despite the similar characteristic as NDD, which is also linearly proportional to N_t . This is important to understand the Δn dependence of rates of LeTID-related reactions [3, 17]. Figure 9 shows generated lifetime as a function of Δn with different values of β and the intrinsic lifetime [43]. The input values that are used for the curve is shown in table 2, which are typical values of industrial solar cells. The error bar is based on the range of k (35 ± 10). The dashed line indicates the one sun equivalent with generation rate, G of $2.67 \times 10^{17} \text{ cm}^{-2} \text{ s}^{-1}$ lifetime. Inset figure shows the Δn at 1 sun (Δn_{1sun}) as a function of β . Above 10^{-3} cm^{-1} of β , Δn_{1sun} is reduced significantly. Considering the typical β_{MDE} is above 10^{-3} cm^{-1} range, Δn_{1sun} is expected to vary up to almost two orders of magnitude. Note that this variation also depends on N_{dop} but

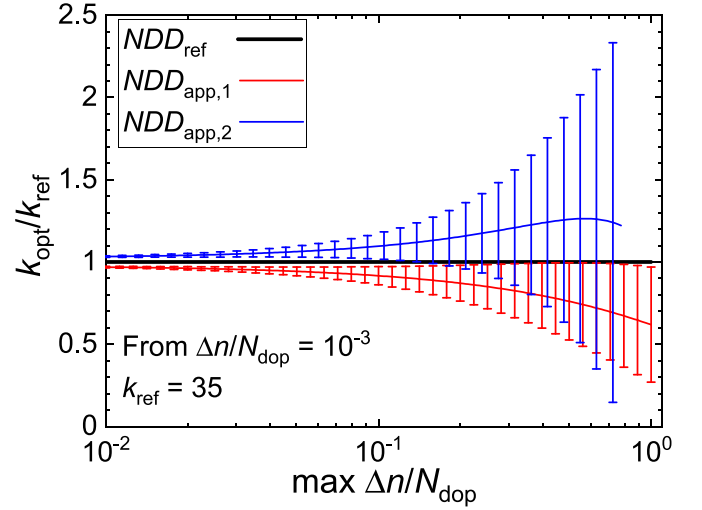


Figure 7. Ratio of optimal k (k_{opt}) to the reference k (k_{ref}) as a function of maximum $\Delta n/N_{dop}$ range on NDD_{ref} , $NDD_{app,1}$, and $NDD_{app,2}$.

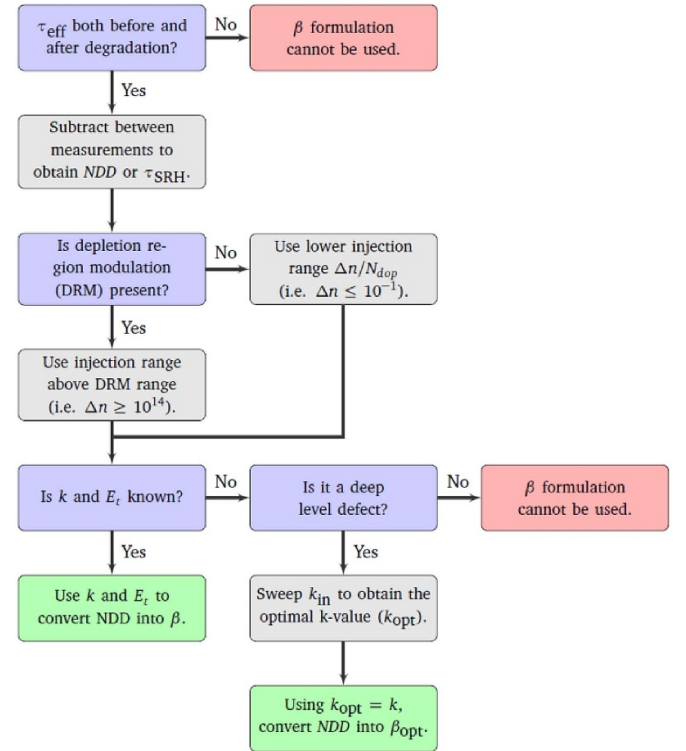


Figure 8. Flow diagram of converting NDD from the measurements to relative defect concentration, β .

considering the N_{dop} is generally high for industrial cells (close to 10^{16} cm^{-3}), this variation of Δn_{1sun} is expected to be similar with different N_{dop} . This application of β is important to quantify the value of Δn at a constant generation rate or an illumination intensity (e.g. one sun) during degradation and recovery of LeTID. Including the recent finding of the temporary recovery of LeTID [44], both the degradation [3, 17] and the recovery [3] from LeTID rates depend on Δn . Therefore, this application is critical to allow simple conversion of Δn

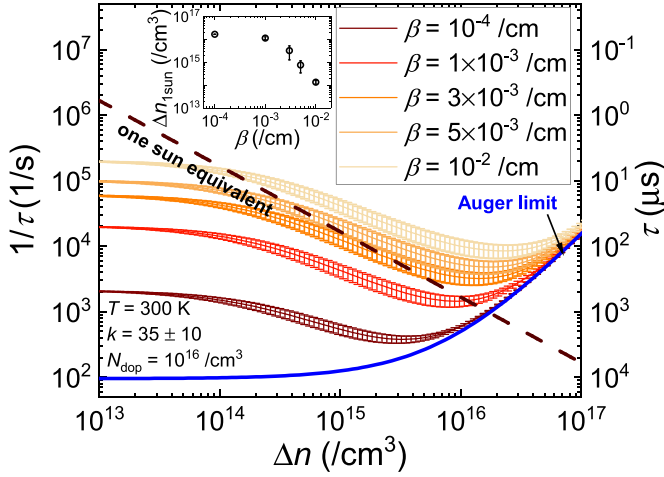


Figure 9. Inverse carrier lifetime (τ) as a function of Δn with different relative defect concentration, β and intrinsic lifetime [43]. Blue line shows the Auger limit based on $N_{\text{dop}} = 10^{16} \text{ cm}^{-3}$ at $T = 300 \text{ K}$ and a dashed line indicates the one sun equivalent lifetime. Error bar is based on k range of 35 ± 10 . Inset shows the Δn at 1 sun ($\Delta n_{1\text{sun}}$) as a function of β .

Table 2. Input parameters for the simulation.

Temperature, T (K)	Background doping density, N_{dop} (cm^{-3})	Thickness of wafer, w (μm)
300	10^{16}	160

variation at a given β , N_{dop} and the starting lifetime at the given generation rate. Increasing the β of BO-LID or LeTID results in a deep level defect that should be independent to the surface lifetime. However, the apparent value of surface lifetime can still be affected at relatively high Δn as when the β or the defect concentration of deep level is significant, τ at Δn can be reduced (typically $\beta > 10^{-3} \text{ cm}^{-1}$ for $N_{\text{dop}} \sim 10^{16} \text{ cm}^{-3}$).

3. Experimental verification using β

The previous section proposed and demonstrated the application of β . In this section, the formulation is applied to experimental results to demonstrate an example of its application in identifying k and converting NDD to β with different base resistivities silicon samples. There will be two experiments (A and B) where two common LID types (BO-LID and LeTID) will be used as an example to identify k and demonstrate its limitation.

3.1. Experimental plan: sample preparations and light soaking condition

This section summarises the sample preparations for the experiments that were performed. Czochralski grown solar-grade mono-crystalline silicon (Cz-Si) wafers or multi-crystalline silicon (mc-Si) wafers both with a resistivity of

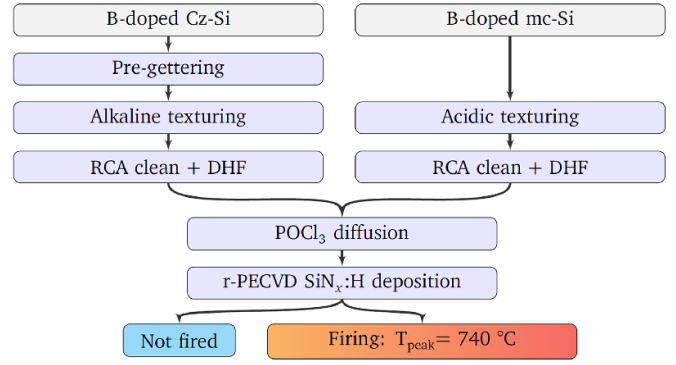


Figure 10. Process flow of the sample preparations for the experiment.

$1.6 \Omega \text{ cm}$ were used. Cz-Si wafers underwent alkaline texturing followed by a pre-gettering process, which involved processed in a tube furnace for 25 mins at 800°C in a POCl_3 ambient followed by a drive-in for 40 min at 880°C in N_2 ambient. The sheet resistance of the emitter was about $65 \Omega/\text{sq}$. This thermal process was followed by a subsequent chemical etch in diluted hydrofluoric (HF) acid ($<3\%$) to remove phosphosilicate glass (PSG) from the wafer surface. Subsequently, they were re-textured in an alkaline solution to etch $2 \mu\text{m}$ from each side of the wafer to remove the getter-diffusion. Pre-gettering in Cz-Si was performed to ensure no significant remaining interstitial iron ($<10^9 \text{ cm}^{-3}$) due to the high concentration of iron in the incoming wafers, which may influence the response to light soaking studies. The initial concentration of iron was over $2 \times 10^{11} \text{ cm}^{-3}$, which is the same type that was used in Hallam et al [45].

Mc-Si wafers underwent standard industrial acidic texturing. Then all wafers went through POCl_3 diffusion, which involved multiple steps: (a) at 795°C with 425 sccm POCl_3 and 600 sccm O_2 for 25 min and (b) 880°C with 7.5 l of N_2 for 40 min to form an n -type emitter of $65 \Omega/\text{sq}$. PSG removal was performed using diluted HF. Hydrogenated silicon nitride ($\text{SiN}_x:\text{H}$) films with a refractive index of 2.08 and thickness of 75 nm were deposited on both sides using plasma-enhanced chemical vapour deposition reactor (Roth and Rau, MAiA) [46] on samples from all experiment groups. Mc-Si wafers then underwent rapid firing at different peak temperatures of 740°C using a commercial infrared firing furnace (Schmid). Figure 10 summarises the process flow for all the samples.

For light soaking conditions, there were two different light sources:

- Light soaking (LS_1) condition: Halogen lamp with 1 kW m^{-2} at 75°C .
- Light soaking LS_2 condition: White LED light source with 0.2 kW m^{-2} at 30°C .

The lamp intensity for halogen lamp and LED is measured using a PM100D power meter and an S350C sensor (Thorlabs) and is reported in kW m^{-2} . For characterisation, the injection-dependent effective lifetime was measured periodically using the quasi-steady state photoconductance (QSSPC)

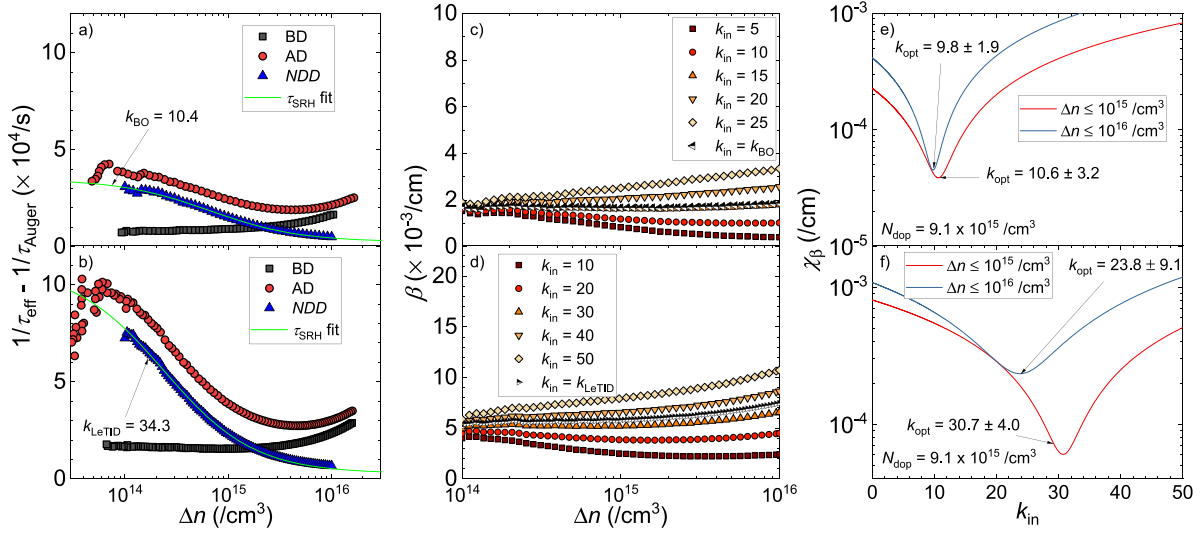


Figure 11. (a) and (b) Inverse effective lifetime ($1/\tau_{\text{eff}}$), and NDD as a function of Δn before (BD) and after degradation (AD). Solid line shows the best fit on NDD curve using τ_{SRH} equation. (c) and (d) β as a function of Δn with different k_{in} . (e) and (f) Standard deviation of β (χ_{β}) as a function of input capture cross-section ratio (k_{in}) with different Δn ranges. Figures (a), (c), and (e) are from Cz-Si and (b), (d), and (f) are from mc-Si.

tool (WCT-120TS, Sinton Instruments) at 30 °C [47] and analysed using the generalised method [48]. The advanced Richter model with Coulomb-enhanced Auger recombination was used [43].

3.2. Identifying the capture cross-section ratios of BO and LeTID defects using β formulation

The experimental work was performed to validate the method of identifying the capture cross-section ratios, k of BO defects and LeTID as examples. The Cz-Si samples were first dark annealed at 250 °C for 1 h, followed by LS₂ condition for 48 h. The dark annealing was done to ensure BO defects are saturated in precursor form without any pre-formation. LS₂ was done to fully transition the precursor form to defect forms, which causes degradation due to BO defects [49]. For mc-Si, the QSSPC measurement was done after firing and after LS₁ for 149 h.

Figures 7(a) and (b) show the inverse effective lifetime after each process and NDD as a function of Δn for Cz-Si and mc-Si, respectively. For each type of wafer, lifetimes before and after the degradation due to light soaking (either LS₁ or LS₂) are subtracted to get NDD as a function of Δn , which are the recombination due to BO defects and LeTID, respectively. The NDD curve is fitted using equation (3), which are shown as solid lines. The k -value due to BO (k_{BO}) and LeTID (k_{LeTID}) were 10.4 and 34.3, respectively. The values are within the range of the reported values from the literature for BO defects [1] and LeTID [24]. Figures 7(c) and (d) show the calculated β as a function of Δn with different k_{in} for Cz-Si and mc-Si, respectively. The plot shows as k_{in} converge to the k -value from figures 11(a) and (b), the β becomes independent to Δn . This characteristic is consistent with the simulated result from figures 4(a) and (b).

Using the β formulation with the assumed value of E_t as mid-gap ($E_g/2$), the calculated β , which was converted from NDD with different k_{in} as a function of Δn , are shown in figures 11(e) and (f). While the k_{opt} based on different Δn ranges from 10^{14} cm^{-3} to 10^{15} cm^{-3} or to 10^{16} cm^{-3} were relatively similar (10.6 ± 3.2 and 9.8 ± 1.9 , respectively), mc-Si showed significantly different k_{opt} (30.7 ± 4.0 and 23.8 ± 9.1). Therefore, the results show that actual k can be determined based on the minimum variation of β (χ_{β}). Using these values, figure 12 shows the β as a function of Δn . For the Cz-Si sample, the variation of β over all Δn when k was only determined from values with a range of Δn below 10^{15} cm^{-3} was slightly higher than that over the larger range. This can be explained by the influenced by the noise at lower Δn around 10^{14} cm^{-3} . For the mc-Si sample, the variation of β was more significant, indicating the larger error due to $\Delta\tau_{\text{other}}$. This is an added benefit of using β as the existence of other changes can easily be recognised and would otherwise go undetected when using NDD, thereby confounding results. While it is not discussed in the study, the approach can also be used to monitor the k as a function of time of the degradation time. When more than one type of LID is present, then apparent value of k is expected to be changed.

The calculated β as a function of Δn using the k_{opt} values from figures 11(e) and (f) are shown in figure 12. Using k_{opt} based on Δn range below 10^{15} cm^{-3} , the β_{opt} based on the average β over Δn for mc-Si and Cz-Si were approximately $(5.6 \pm 0.5) \times 10^{-3} \text{ cm}^{-1}$ and $(1.7 \pm 0.1) \times 10^{-3} \text{ cm}^{-1}$, respectively where the value of mc-Si was similar to the typical values from other studies mentioned in figure 3. Nevertheless, the k -values of BO and LeTID defects in Cz-Si and mc-Si, respectively that are identified using k_{opt} are in a good agreement with the k -value from Bothe *et al* [1] for BO defects and from Niewelt *et al* for LeTID [21]. It is important to note that one study reported BO defects may not be due to SRH

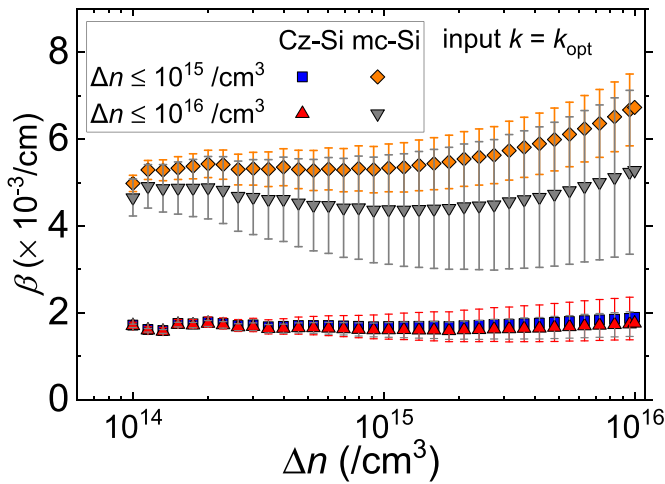


Figure 12. Relative defect concentration, β using optimal k , k_{opt} from different Δn ranges as a function of Δn for Cz-Si and mc-Si.

recombination [50]. However, the result still demonstrates the application of β on identifying k with assumption of a single type of deep level defect and the trap-assisted Auger recombination generally obeys SRH statistics.

The approach shown here is mainly applicable for a single defect. When more than one type of LID is present, for example BO-LID and LeTID in boron-doped Cz silicon [39, 40], it is possible for the multiple defects to influence the overall value of k with an assumption of a single defect. The variation of β as a function of Δn during the degradation and recovery with a fixed input k is expected to be unchanged for a single defect. Therefore, it can also be an approach to identify a potential influence of more than one defect. Nevertheless, in order to isolate or identify the influence of other effects, the samples must be prepared cautiously in advance or treated carefully to prevent the influence. Even with potential errors in k , the variation in β across the injection levels is still substantially smaller than that expected for NDD with the variation of approximately 6 and 16 for the Cz-Si and mc-Si, respectively, over the range of Δn from 10^{14} cm^{-3} to 10^{16} cm^{-3} . This demonstrates that the methods are applicable to identify the defect parameters experimentally and the benefit of using β . Our future study will investigate the temperature dependent measurements to improve the accuracy of the method.

4. Conclusion

This paper introduced a term for the relative defect concentration, β , to correct the pitfall of NDD. This term overcomes issues with the use of NDD, which varies with both Δn and N_{dop} . For example, using $k = 35$ for LeTID, NDD can vary by a factor of 3 over the range of Δn between 10^{14} cm^{-3} and 10^{15} cm^{-3} . On the other hand, when β is used for a defect with known k , it is theoretically injection-level independent. As such, it overcomes the need to use a specific $\Delta n/N_{\text{dop}}$ ratio and enables direct comparison between the

maximum concentration of defects due to LID, mainly BO-LID and LeTID defects with different samples from different studies. Based on the literature results, while the NDD at the MDE extents varied over an order of magnitude, the majority of the studies showed the value of β is in the range of $(1-10) \times 10^{-3} \text{ cm}^{-1}$. Based on the calculation, when N_{dop} is high, 10^{16} cm^{-3} , for example, the variation of Δn due to LeTID with this amount of β is expected to be almost two orders of magnitude. Furthermore, the single value of β obtained is directly proportional to the true defect concentration. Using β , the error from the experiment results was reduced to below 12% where the uncertainty was due to change in surface lifetime.

Another application of β is that it can be used to identify the capture cross-section ratio, k , of deep-level defects, based on the injection-level independent property. This only holds for the correct value of k , and hence can be obtained by minimising χ_{β} , the standard deviation of β over a given range of Δn . Based on the experimental results and the proposed method, the k -value of the defects due to BO-LID and LeTID identified were 10.6 ± 3.2 and 30.7 ± 4.0 , respectively, which are consistent with the values from the literature, thereby validating the method. This approach can have a universal application to compare defect concentrations that are directly comparable and also identify the k -value of unknown impurities. Using the k -value, the β of LeTID for mc-Si and BO-LID for Cz-Si were approximately $(5.6 \pm 0.5) \times 10^{-3} \text{ cm}^{-1}$ and $(1.7 \pm 0.1) \times 10^{-3} \text{ cm}^{-1}$, respectively where the value for the LeTID was similar to the typical values from other studies.

Data availability statement

All data that support the findings of this study are included within the article (and any supplementary files).

Acknowledgments

The support of the Australian Government through the Australian Renewable Energy Agency (ARENA, 2017/RND005, 1-SRI001, 1-060) and Australian Centre for Advanced Photovoltaics (ACAP) is acknowledged. The views expressed herein are not necessarily the views of the Australian Government, and the Australian Government does not accept responsibility for any information or advice contained herein. The authors acknowledge the Solar Industrial Research Facility (SIRF) for provision of facilities and equipment used for characterization. B H would like to acknowledge the support of the Australian Research Council (ARC) through a Discovery Early Career Researcher Award (DE170100620) and PhD scholarship for M K M K would like to also acknowledge the support of ACAP for his fellowship.

ORCID iD

Moonyong Kim  <https://orcid.org/0000-0002-3860-5633>

References

- [1] Bothe K and Schmidt J 2006 *J. Appl. Phys.* **99** 013701
- [2] Rein S and Glunz S W 2003 *Appl. Phys. Lett.* **82** 1054–6
- [3] Kersten F et al 2015 *Sol. Energy Mater. Sol. Cells* **142** 83–86
- [4] Eberle R, Kwapil W, Schindler F, Glunz S W and Schubert M C 2017 *Energy Proc.* **124** 712–7
- [5] Bredemeier D, Walter D C and Schmidt J 2018 *AIP Conf. Proc.* **1999** 130001
- [6] Yli-koski M, Serué M, Modanese C, Vahlman H and Savin H 2019 *Sol. Energy Mater. Sol. Cells* **192** 134–9
- [7] Glunz S W, Rein S, Lee J Y, Warta W, Glunz S W, Rein S, Lee J Y and Warta W 2001 *J. Appl. Phys.* **90** 2397–404
- [8] Herguth A 2019 *IEEE J. Photovoltaics* **9** 1182–94
- [9] Shockley W and Read W T 1952 *Phys. Rev.* **87** 835–42
- [10] Cuevas A, Member S, Stocks M, Macdonald D, Kerr M and Samundsett C 1999 *18th IEEE Photovolt. Spec. Conf.* pp 2026–34
- [11] Macdonald D and Cuevas A 2001 *J. Appl. Phys.* **89** 7932–9
- [12] Green M A 1990 *J. Appl. Phys.* **67** 2944–54
- [13] Glunz S W, Rein S, Warta W, Knobloch J and Wettling W 2001 *Sol. Energy Mater. Sol. Cells* **65** 219–29
- [14] Bothe K, Hezel R and Schmidt J 2004 *Solid State Phenom.* **95–96** 223–8
- [15] Eberle R, Kwapil W, Schindler F, Schubert M C and Glunz S W 2016 *Phys. Status Solidi* **10** 861–5
- [16] Bredemeier D, Walter D C, Heller R and Schmidt J 2019 *Phys. Status Solidi* **13** 1900201
- [17] Kwapil W, Niewelt T and Schubert M C 2017 *Sol. Energy Mater. Sol. Cells* **173** 80–84
- [18] Herguth A 2019 *Phys. Status Solidi* **216** 1900322
- [19] Varshney U, Abbott M, Ciesla A, Chen D, Liu S, Sen C, Kim M, Wenham S, Hoex B and Chan C 2019 *IEEE J. Photovoltaics* **9** 601–7
- [20] Liu S et al 2018 *IEEE J. Photovoltaics* **8** 1494–502
- [21] Niewelt T, Selinger M, Grant N E, Kwapil W, Murphy J D and Schubert M C 2017 *J. Appl. Phys.* **121** 185702
- [22] Sperber D, Heilemann A, Herguth A and Hahn G 2017 *IEEE J. Photovoltaics* **7** 463–70
- [23] Bredemeier D, Walter D and Schmidt J 2017 *Sol. Energy Mater. Sol. Cells* **173** 2–5
- [24] Chen D et al 2017 *Sol. Energy Mater. Sol. Cells* **172** 293–300
- [25] Kersten F, Heitmann J and Müller J W 2016 *Energy Proc.* **92** 828–32
- [26] Macdonald D H, Geerligs L J and Azzizi A 2004 *J. Appl. Phys.* **95** 1021–8
- [27] Kim M, Chen D, Abbott M, Nampalli N, Wenham S, Stefani B and Hallam B 2018 *J. Appl. Phys.* **123** 161586
- [28] Jensen M A, Morishige A E, Hofstetter J, Needleman D B and Buonassisi T 2017 *IEEE J. Photovoltaics* **7** 980–7
- [29] Sperber D, Herguth A and Hahn G 2017 *Phys. Status Solidi* **11** 1600408
- [30] Vargas C, Zhu Y, Coletti G, Chan C, Payne D, Jensen M and Hameiri Z 2017 *Appl. Phys. Lett.* **110** 092106
- [31] Winter M, Walter D, Bredemeier D and Schmidt J 2019 *Sol. Energy Mater. Sol. Cells* **201** 110060
- [32] Niewelt T, Mägdefessel S and Schubert M C 2016 *J. Appl. Phys.* **120** 085705
- [33] Hallam B, Abbott M, Nærland T and Wenham S 2016 *Phys. Status Solidi* **10** 520–4
- [34] Bredemeier D, Walter D C and Schmidt J 2017 *Sol. RRL* **2** 1700159
- [35] Niewelt T, Schön J, Schindler F and Schubert M C 2017 *Prog. Photovoltaics Res. Appl.* **26** 533–42
- [36] Murphy J D, Bothe K, Krain R, Voronkov V V and Falster R J 2012 *J. Appl. Phys.* **111** 113709
- [37] Nampalli N, Fung T H, Wenham S, Hallam B and Abbott M 2017 *Front. Energy* **11** 4–22
- [38] Macdonald D, Roth T, Deenapanray P N K, Bothe K, Pohl P and Schmidt J 2005 *J. Appl. Phys.* **98** 083509
- [39] Fertig F et al 2017 *Energy Proc.* **124** 338–45
- [40] Kim M, Chen D, Abbott M, Wenham S and Hallam B 2018 *AIP Conf. Proc.* **1999** 130010
- [41] Cousins P J, Neuhaus D H and Cotter J E 2004 *J. Appl. Phys.* **95** 1854–8
- [42] Bardos R A, Trupke T, Schubert M C and Roth T 2006 *Appl. Phys. Lett.* **88** 1–3
- [43] Richter A, Glunz S W, Werner F, Schmidt J and Cuevas A 2012 *Phys. Rev. B* **86** 165202
- [44] Krugel G, Wolke W, Geilker J, Rein S and Preu R 2011 *Energy Proc.* **8** 47–51
- [45] Hallam B, Chen D, Kim M, Stefani B, Hoex B, Abbott M and Wenham S 2017 *Phys. Status Solidi* **214** 1700305
- [46] Hameiri Z, Borojevic N, Mai L, Nandakumar N, Kim K and Winderbaum S 2017 *IEEE J. Photovoltaics* **7** 996–1003
- [47] Sinton R A, Cuevas A and Stuckings M 1996 *Conf. Rec. Twenty Fifth IEEE Photovolt. Spec. Conf.—1996* (IEEE) pp 457–60
- [48] Nagel H, Berge C and Aberle A G 1999 *J. Appl. Phys.* **86** 6218
- [49] Kim M, Abbott M, Nampalli N, Wenham S, Stefani B and Hallam B 2017 *J. Appl. Phys.* **121** 053106
- [50] Vaqueiro-Contreras M, Markevich V P, Coutinho J, Santos P, Crowe I F, Halsall M P, Hawkins I, Lastovskii S B, Murin L I and Peaker A R 2019 *J. Appl. Phys.* **125** 0–16